20th IMEKO TC4 International Symposium and
18th International Workshop on ADC Modelling and Testing
Research on Electric and Electronic Measurement for the Economic Upturn
Benevento, Italy, September 15-17, 2014

A Low-cost Ultrasonic Rangefinder based on Frequency Modulated Continuous Wave

Luigi Battaglini, Pietro Burrascano, Alessio De Angelis, Antonio Moschitta, and Marco Ricci*

Department of Engineering, Polo Scientifico e Didattico di Terni, University of Perugia,
Strada di Pentima 4, 05100 Terni, Italy;
*corresponding author: marco.ricci@unipg.it

Abstract – In the present work the performance of a low-cost ultrasonic rangefinder system exploiting linear chirp excitation signal and the Frequency Modulated Continuous Wave technique is analyzed, evaluated in terms of resolution and computational cost, and compared with the results achievable by means of the standard technique based on the matched-filter theory. The system, based on a Voltage Controlled Oscillator and an analog mixer, shifts some of the processing required by the FMCW protocol in the analog domain, strongly relaxing the requirements on the signal sampling rate without reducing the achievable range resolution. The final target is to evaluate the possibility of implementing the FMCW technique in very low cost and hand held devices.

Keywords: NDT, FMCW, Ultrasonic, Sub-sampling.

I. INTRODUCTION

Time of Flight (*ToF*) evaluation is a central issue in several measurement schemes that involve ultrasonic rangefinding systems, such as obstacle detection for automotive applications or positioning [1]. In particular, since the measurements are usually performed in a noisy environment and, at the same time, the hardware and the software costs should be reduced as much as possible, it is of utmost importance to compare and evaluate different measurement schemes and to characterize their performances, possibly relaxing any requirements on hardware characteristics and Digital Signal Processing complexity. In this scenario, the Frequency Modulated Continuous Waveform (FMCW) protocol could be a suitable choice. FMCW is a well-known technique developed for radar and optic applications [2-4] and in the last decade it was adopted several times in ultrasonic field [5-7]. With respect to more standard approaches in ultrasonic *ToF* measurement schemes such as Pulse-Echo [8] and Pulse compression [9],[10],[11], FMCW presents peculiar characteristics that can provide useful benefits in real-world applications. In particular, in this paper it will be shown how by using this procedure most of the processing can be easily realized using low-cost hardware, and also how the sampling rate can be significantly reduced, still preserving the range resolution. The basic idea is that mixing a linear chirp with a delayed replica results in a signal with low frequency components that can easily be separated from high frequency content using a simple analog filter, the low frequency part depending on the delay between the two chirps. To this aim a specific hardware has been designed, using off-the-shelf analog components. In particular, ultrasound transceivers have been used, to generate and receive a chirp signal linearly spanning the 35-47.5 kHz frequency range, and the low frequency component has been acquired with a sampling rate ranging from 500 kHz to the chirp bandwidth of 12.5 kHz. A comparison has been done between classic pulse compression techniques and the FMCW technique in order to define the trade-offs involved by the two approaches as a function of the adopted sampling rate.

II. THEORY

The FMCW method, summarized in Fig. 1 involves mixing a pulse train of linear chirps with a similar train, delayed and possibly distorted by the propagation medium. Let us assume a simplified scenario, consisting in two probes, put at a distance *d* and facing each other. The measurement process starts with the excitation of an

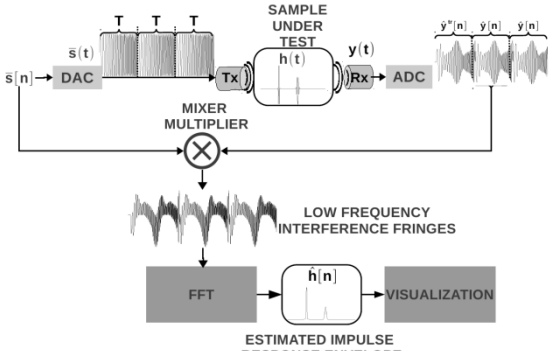

Fig. 1. Schematic approach for FMCW analysis

emitting ultrasound transducer Tx with a periodic chirp signal $s(\cdot)$, sweeping in a frequency interval $[f_0,f_1]$ in a time T, obtained by feeding a D/A converter with a proper digital sequence $s[\cdot]$. The emitted ultrasonic signal $y(\cdot)$, propagates in the medium, hereby assumed not frequency selective, and enters the receiving transducer

ISBN-14: 978-92-990073-2-7

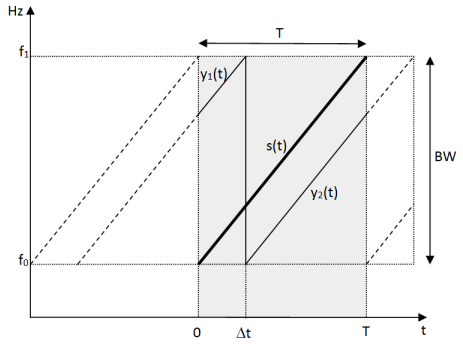

Fig. 2. Frequency-time relation between signals.

Rx, bringing information about the medium, such as the propagation delay Δt. The instantaneous frequencies of both $s(\cdot)$ and $y(\cdot)$ are shown in the spectrogram of Fig. 2, as a function of time.

If $y(\cdot)$ is acquired using an A/D converter (ADC), the obtained sequence $y[\cdot]$ can be sample-by-sample multiplied with $s[\cdot]$, approximating the product

$$\chi(t)=s(t)y(t), \quad (1)$$

shown in Fig. 3. The mixed signal $\chi(\cdot)$ brings information about the propagation medium, such as the Impulse Response (IR) and especially the propagation delay, required for *ToF* measurement purposes. As an architectural alternative, the received signal $y(\cdot)$ can be mixed in the analog domain with $s(\cdot)$.

It is well known that mixing two sinewaves at frequencies $f_a<f_b$ provides two signals, a sinewave with a low frequency f_b-f_a, and a high frequency sinewave, with a frequency f_b+f_a. In presence of chirp signals, approximately the same relations hold but for the instantaneous frequencies of $f_s(t)$ and $f_y(t)$, which change in time. Two components therefore are produced as before but while the lower frequency component $f_y(t)$-$f_s(t)$ is constant, the higher one $f_y(t)$-$f_s(t)$ changes in time with a rate double with respect the original chirp. However, as shown in Fig. 2, it is worth to stress that, due to the periodicity of the chirp signal employed, two different overlapping regions exist between the instantaneous frequencies of the transmitted and the received signals. This means, from a practical point of view, that in each period T two different time regions should be considered associated at two -in general distinct- low-frequency beats generated by the mixing. These beats can be identified by analyzing the spectral content of $\chi(\cdot)$ using the Discrete time Fourier Transform (*DFT*). Moreover the high frequency component of the mixer output is a chirp as well. Its frequency ranges approximately in the [$2f_0$, $2f_1$] interval. Thus, at a given time t, the mixer output ultimately features the following components, shown in Fig. 4:

- A low-frequency sinusoid due to the first zone of overlapping between sent and acquired signal, at frequency $f_1=\Delta t\times(BW/T)$ corresponding to $f_y(t)$-$f_s(t)$= $f_s(t+\Delta t)$-$f_s(t)$;
- Another low-frequency sinusoid due to the second zone of overlapping between sent and acquired signal, at frequency $f_2=(T-\Delta t)\times(BW/T)$ corresponding to $f_y(t)$-$f_s(t)$= $f_s(t+T-\Delta t)$-$f_s(t)$= $f_s(t-\Delta t)$-$f_s(t)$;
- A chirp signal with double frequency characteristics with respect to the sent chirp.

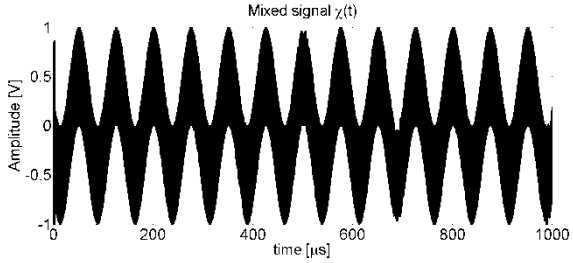

Fig. 3.Signal after point-by-point multiplication.

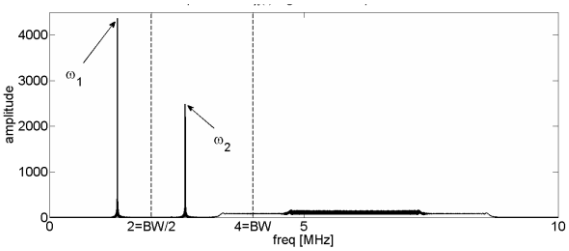

Fig. 4. DFT of the mixer output

Notice that, by analyzing the mixer instantaneous frequency, it can also be proven that:

$$f_1 + f_2 = BW \quad (2)$$

as can be intuitively verified by looking at Fig.2.

III. EXPERIMENTAL IMPLEMENTATION

The previous theoretical model has been used to perform several measurements of distance with the help of a plotter scan that allows varying the distance between sending and acquiring probe. The characterization was performed by transmitting the ultrasound signal in air, taking 10 measurements in each position, and using the results to extract statistics and evaluate some performance metrics. For each position, the developed system, described in subsection III.A, saved: transmitted signal, acquired signal, mixer output, acquisition rate, *ToF* statistics, signal spectra and external controls[1].

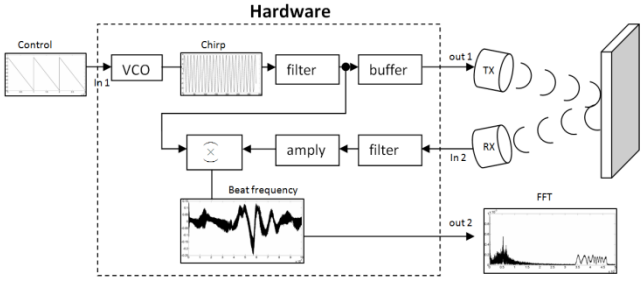

Fig. 5. Schematic layout of the hardware device.

[1] The signal has been generated with a VCO component, while multiplication has been performed externally by a mixer component, see Section III.A for more details.

By this way, together with the FMCW analysis, also an estimation of the *ToF* via matched filter techniques can be executed, as needed to perform a comparison of the two approaches. The system low frequency output has been analysed using various techniques, under various conditions. Both the considered configurations and the *ToF* estimation algorithms are described in section III.B.

Layout and hardware apparatus

Fig. 5 shows the layout of the analog processing hardware, capable of generating a linear chirp, transmitting the signal, receiving it, and mixing it with the transmitted chirp pulse train.

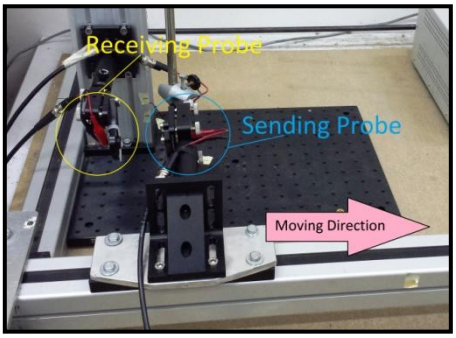

Fig.6 Laboratory set-up.

In particular the system includes a Voltage Controlled Oscillator (VCO), whose instantaneous frequency is controlled by an external voltage signal. Thus, by driving the VCO with a saw-tooth signal it outputs a periodic pseudo-chirp signal that is a rectangular pulse train with variable frequency. The pseudo-chirp signal is low-pass filtered (F_c=70kHz) to eliminate the 3rd harmonic typical of the square wave, and any higher unwanted component, in order to obtain a signal as close as possible to an ideal chirp. After that, the signal is split, feeding both the TX element, after a buffering to prevent load effects, and one of the mixer inputs. Conversely, the received signal is bandpass filtered, removing unwanted spectral content outside the [10÷100 kHz] band, amplified, with a gain of 1.875, and sent to the second mixer input.

Set-up and signals

The scanning setup, shown in Fig. 6, was used to generate and acquire several signals, with the following parameters:

- measurement range: 50÷560 mm
- number of steps: 170 (resolution 3mm)
- propagation medium: air
- acquisition rate: [500, 200, 100, 12.5] kHz
- chirp bandwidth BW: 12.5 kHz
- chirp start frequency f1: 35kHz
- chirp period T: 100ms

Fig.7 shows the transmitted signal (a), the acquired signal (b) and the mixer output (c), obtained for a fixed distance between the transmitter and the receiver of 300 mm. Fig. 7(d) shows the Impulse Response (IR), i.e. the correlation sequence obtained using matched filtering, while Fig. 7(e) shows the *DFT* spectrum of the $\chi(\cdot)$ mixer output, obtained using Fast Fourier Transform algorithm.

It can be seen that the peak frequency of the mixer output spectrum changes as well as the correlation peak, as a function of *d*. The FMCW approach transforms therefore a measure of time in a measure of frequency, and this can be a great advantage when very small time delay have to be measured (e.g. in optics or in radar). On the other hand, the weakness of this approach results to be the measurement resolution, limited by the width of a *DFT* frequency bin, that can be reduced only by taking long acquisitions. Two different solution has been tested to relax such requirement:

- Chirp Z-Transform algorithm (*CZT*) [12].
- Parabolic analytical interpolation model (INT) to define the beat frequency by exactly fitting a parabola to three points: the maximum detected by *DFT*, the previous *DFT* frequency bin, and the next one [13].

Both approaches were implemented, and the resulting

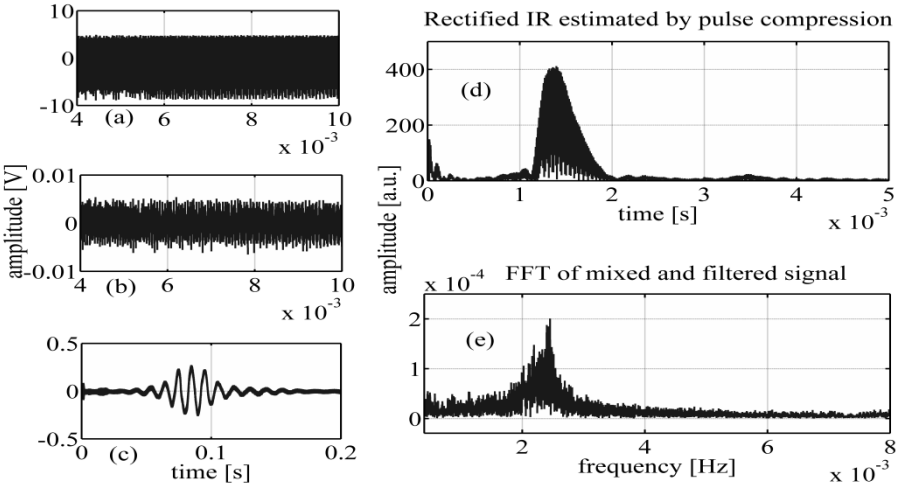

Fig.7. Measured and processed signals. IR stands for impulse response

ToF estimations were compared with the traditional pulse compression method.

IV. RESULTS

The low-frequency beat has been acquired at different acquisition rates, using the proposed algorithms for various sampling approaches. In particular, Fig. 8 shows the estimated distance, obtained by converting the underlying *ToF* estimations, as a function of the actual distance *d*, for a sampling frequency of 500 ksample/s. Fig. 8(A) has been obtained using the standard pulse compression (i.e., correlation techniques), Fig.8(B) was obtained using *DFT* evaluation, Fig. 8(C) was obtained using the *CZT* transformation and Fig. 8(D) has been obtained by applying parabolic interpolation to the *DFT* results. Similarly, Fig. 9 has been obtained for a sampling rate of 12,5 kSample/s. These two measurements are shown because their sample rates are the limit values of the chosen acquisition rates to investigate.

For each technique, a best fit line was obtained, by applying the Least Square (LS) method to the data points. Then, the global error GE, defined as the summation of the distance of each point from the best fit straight line, was evaluated for each algorithm, and used as indicator of the measurement precision. The LS method allows the computation also of the experimental standard deviation σ of the range measurement, that, assuming an underlying Gaussian distribution, defines the confidence interval with a 68.3% probability of confidence. These two parameters consent to compare different measurements, assessing their precision and accuracy. The analysis results are summarized in the following Table I for sampling rates that vary from 500 ksample/s to 12,5 ksample/s. The range resolution values achieved, i.e. the σ values, are well beyond the intrinsic expected resolution σ_{EX} that can be assumed inversely proportional to the signal bandwidth: σ_{EX} (in air) = (v_{air} BW^{-1})/2 ~ 13 mm. In particular, it can be observed that the *CZT* and the *DFT* interpolation are seemingly the most promising approaches, offering both the minimum GE and σ, and reaching quite good resolution values despite the narrowband feature of the transreceivers used. Moreover the FMCW approach demonstrates experimentally to be robust against reduction of sampling frequency as expected by the theory.

In fact, the *DFT* resolution is determined only by the duration of the acquisition and, having maintained constant the acquisition duration for all the tests, the performance of the *DFT* method is approximately constant with respect to the sampling rate used , as shown in Table I. Conversely, this is not true for the *ToF* method based on the matched filter approach.

By lowering the sampling rate, and then increasing the temporal quantization step, the performance of the *ToF* approach is expected to decrease. Nevertheless, quite surprisingly, the *CZT* and *DFT* interpolation obtain better results then standard matched filter approach even at the highest sampling rate, where the *ToF* should exhibit the highest resolution. How it is can be explained? As said the *DFT*-based methods resolution depends uniquely on the duration while for the *ToF* approach the resolution increases as the sampling rate increases. In an ideal noiseless word, the lower limit resolution of *ToF* is simply the sampling time: $\sigma_{ToF} < R^{-1}$ while that of the *DFT* is actually given by the expression $\sigma_{FFT} < T^{-1} \times (T/BW) = BW^{-1}$.

Since the minimum sampling rate that can be used in the FMCW protocol is B, the *ToF* lower resolution always overperforms the *DFT*. Nonetheless experimental results show that the actual *DFT* resolution equals approximately that of the *ToF* at the highest rate used while it is better if a subsampling is applied. Furthermore *DFT*-derived methods, *CZT* and INT, enhance the resolution of *DFT* and therefore are better then *ToF* at any rate. We hypotize that this quite unexpected result is due to various factors such as the effect of noise, the spectral behavior of the transreceivers, the different processing and to the different way by which the signal are acquired. Regarding the processing, *ToF* is individuated by taking the instant at which the maximum of the Impulse Response envelope occurrs. Noise affect this signal and therefore the maximum can be found at a time instant different from the expected one. Moreover, since the envelope is calculated from digital signals, some mathematical noise can arise, especially for low sampling rates. These two combined effects lead to a dispersion of the *ToF* values measured even when a measure is reapeted several times. Furthermore, since the bandwidth of the transducers is limited, the envelope of the impulse response even in the

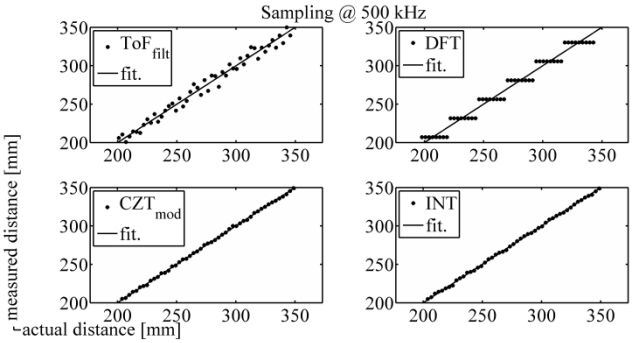

Fig. 8. Comparison among Pulse compression, DFT, CZT and Interpolation @500 kHz.

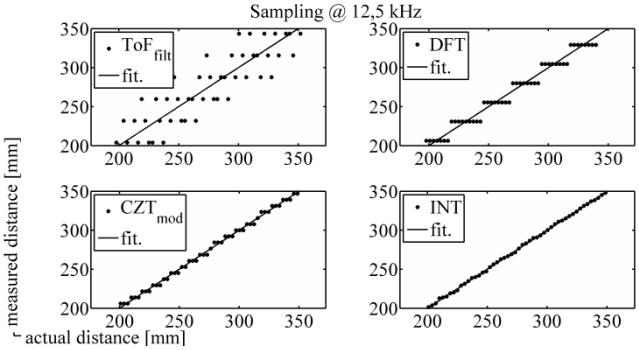

Fig. 9. Comparison among Pulse compression, DFT, CZT and Interpolation @12,5 kHz.

case of a simple time-delay between Tx and Rx presents a wide main lobe which width actually regulates the dispersion of the *ToF* values.

On the other hand, *DFT* and *CZT* applied to the mixed signals directly return the envelope of the IR from which the *ToF* is retrieved by taking the frequency at which the maximum happens and then applying a proper scaling factor (T/BW). By looking at the collected data, the envelope retrieved by frequency methods is less noisy than the one obtained by the matched filter approach, implying a smaller spread of the distance measured values, see Fig. 10.

Moreover it should be taken into account that the *ToF* IR is obtained starting from the sampled signals s[n] and y[n] while the *DFT*/*CZT* are calculated on χ[n] signal that is sampled after the analog mixing of y(t) and s(t) and the application of a low-pass filtering capable of removing the high-frequency component: this fact may improve the resolution of the *DFT*-based methods especially at lower sampling rates.

	500 ksample/s *N*=100000		200 ksample/s *N*=40000		100ksample/s *N*=20000		12,5ksample/s *N*=2500	
	GE [mm^2]	σ [mm]	GE [mm^2]	σ [mm]	GE [mm^2]	σ [mm]	GE [mm^2]	σ [mm]
ToF	2027	6,30	4004	8,86	7336	12,00	27000	23,00
DFT	2621	7,16	2665	7,23	2562	7,08	2572	7,10
CZT	56	1,04	36	0,83	77	1,22	353	2,63
INT	69	1,16	87	1,30	67	1,14	66	1,13

Table 1. GE and σ for different sampling rates, *N* is the number of acquired samples.

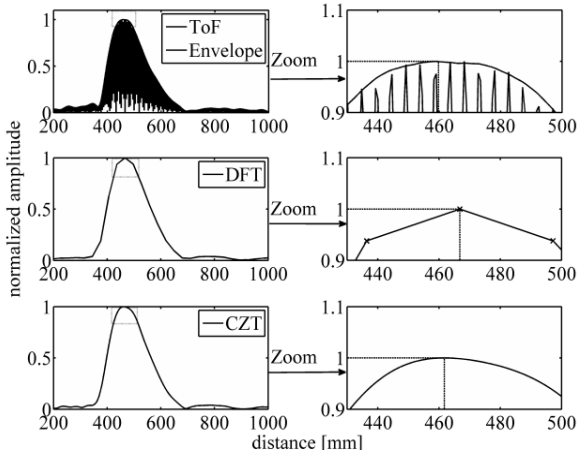

Fig. 10. Typical examples of IR envelopes retrieved by (up) Matched Filter, (middle) DFT, (bottom) CZT. On the right column are reported the zooms of the signals around the relative peaks: it can be seen that for the ToF case in the peak region several local maxima are present. In DFT and CZT cases the peak is instead uniquely determined.

V. CONCLUSIONS

The presented work shows that is possible to perform accurate distance measurements with FMCW techniques also when only a low sampling rate can be applied, due to constraints on components cost and performance. The *CZT* and the *DFT* parabolic interpolation seem to be the most precise and accurate techniques, especially when the sampling frequencies and the record length assume low values.

References

[1] A. De Angelis, A. Moschitta, P. Carbone, M. Calderini, S. Neri, R. Borgna, M. Peppucci, "Design and characterization of an ultrasonic indoor positioning technique," Proc. of 2014 IEEE Instrumentation and Measurement Technology Conference I2MTC 2014, Montevideo, Uruguay, May 12 – 15, 2014.

[2] A. Stove, "Linear FMCW radar techniques," IEE Proceedings Radar and Signal Processing, Vol. 139, no. 5, 1992.

[3] J. Zheng, "Analysis of Optical Frequency-Modulated Continuous-Wave Interference," Applied Optics, vol. 43, 2004.

[4] J. Zheng, Optical Frequency-Modulated Continuous-Wave (FMCW) Interferometry, Springer, 2005.

[5] M. Kunita et al. "Range measurement using ultrasound FMCW signals," IEEE Ultrasonics Symposium, 2008, pp. 1366-1369, 2008.

[6] O. P. Sahu, A. K. Gupta, "Measurement of Distance and Medium Velocity," IEEE Trans. Instrument. Meas., vol. 57, no. 4 pg. 838-842, 2008.

[7] L. Battaglini, M. Ricci and L. Senni "Frequency Modulated Continuous Wave Ultrasonic Radar," Int.l Conf. on Digital Signal Processing, Santorini, 2013.

[8] S. Natarajan, et al "Accurate step-FMCW ultrasound ranging and comparison with pulse-echo signaling methods." SPIE Medical Imaging, 2010.

[9] G. Turin, "An Introduction to Matched Filters," IRE Trans., pp. 311-239, 1960.

[10] F. Lam, F. Szilard, "Pulse compression techniques in ultrasonic non-destructive testing," Ultrasonics, vol. 14, no. 3, pp. 111-114, 1976.

[11] M. Ricci et al., "Pulse-compression ultrasonic technique for the inspection," Insight - Non-Destructive Testing and Condition Monitoring, vol. 54, no. 2, 2012.

[12] Rabiner, L., Schafer, R. W., & Rader, C. M. (1969). The chirp z-transform algorithm. Audio and Electroacoustics, IEEE Transactions on, 17(2), 86-92.

[13] Svilainis, L., Lukoseviciute, K., Dumbrava, V., & Chaziachmetovas, A. " Subsample interpolation bias error in time of flight estimation by direct correlation in digital domain" Measurement, 46(10), 3950-3958,2013.